A Jahn-Teller study of the orthorhombically distorted Cr^{2+} centre in SrF_2 and CaF_2

1999 J. Phys.: Condens. Matter 11 2579

(http://iopscience.iop.org/0953-8984/11/12/012)

J. Phys.: Condens. Matter **11** (1999) 2579–2588. Printed in the UK PII: S0953-8984(99)96582-7

A Jahn–Teller study of the orthorhombically distorted Cr^{2+} centre in SrF_2 and CaF_2

P B Oliete†‡, C A Bates† and J L Dunn†

† School of Physics and Astronomy, University of Nottingham, University Park, Nottingham NG7 2RD, UK

‡ Instituto de Ciencia de Materiales de Aragón, Universidad de Zaragoza–Consejo Superior de Investigaciones Científicas, Plaza San Francisco s/n, E-50009 Zaragoza, Spain

Received 6 August 1998

Abstract. Cr^{2+} centres in SrF_2 and CaF_2 are strongly coupled Jahn–Teller systems. A theoretical Jahn–Teller model is developed, in which the parameters that appear in the effective Hamiltonian describing the $^5T_{2g}$ ground state of the Cr^{2+} ion are obtained by fitting previously published EPR results. It is found necessary to include certain random strains in the analysis in order to explain the orthorhombic features of the EPR spectra. The coupling between the ground and excited states and the effects of other perturbations are discussed.

1. Introduction

Divalent chromium in tetrahedral environments has been the subject of numerous experimental studies. (See [1] for an earlier review.) In many systems, the orbital degeneracy of the $^5T_2$ ground state appears to be lifted as the ions show a tetragonal distortion. Such systems include Cr^{2+} centres in II–VI and III–V semiconductor matrices, which are the best known examples of tetragonally distorted Cr^{2+} ions in the literature. These studies include electron paramagnetic resonance (EPR) experiments on the III–V semiconductors GaAs [2] and InP [3] and on II–VI semiconductors [4, 5]. The original studies of Cr^{2+} in GaAs proposed that the tetragonal nature of the spectra corresponded to a static $T_2 \otimes e$ Jahn–Teller (JT) effect [2, 6]. However, in real systems a static JT effect does not exist as perturbations cause the system to tunnel between equivalent minima. Consequently, Abhvani *et al* [7] developed a detailed theoretical model in which all of the experimental results (including EPR, acoustic paramagnetic resonance (APR) and phonon scattering measurements) could be explained in terms of a strain-stabilized dynamic JT effect.

Cr^{2+} systems in eightfold coordination have been studied in much less detail although some results have been reported on divalent chromium in alkaline earth halides. The only optical experiments reported are an absorption study of Cr^{2+} impurities in CdF_2 [8]. More recently, some continuous wave (CW) and pulsed EPR studies have been undertaken. For example, the EPR spectra from Cr^{2+} centres were found to reflect a tetragonal symmetry in BaF_2 and $SrCl_2$ [9]. However, the Cr^{2+} centres exhibited orthorhombic symmetry in SrF_2 [10, 11], in CaF_2 [12] and in CdF_2 [13]. The origin of the tetragonal distortion for Cr^{2+} centres in BaF_2 could be due to an off-centre ion [14] although this is not clear. For the orthorhombic case, the origin of the distortion has been successfully assigned to a $T_{2g} \otimes (e_g + t_{2g})$ JT effect in the papers cited. Whilst the experimental data has been analysed in terms of a spin Hamiltonian for a

0953-8984/99/122579+10$19.50

non-degenerate orbital state with electron spin $S = 2$, no calculations have been attempted in terms of a more basic description. The reason is that an appropriate theoretical model is absent.

The aim of this work is to develop a theoretical JT model for orthorhombic Cr^{2+} centres in SrF_2 and CaF_2. An effective Hamiltonian will be constructed in order to describe these ions in terms of a strong dynamic JT effect with strain stabilization. This will allow all the experimental features observed in the published EPR results to be explained.

2. Summary of the experimental results and a spin Hamiltonian model

As stated above, CW and pulsed EPR studies of Cr^{2+} in SrF_2 and CaF_2 have been recently reported. In both cases, an anisotropic spectrum was obtained, corresponding to an ion in orthorhombic symmetry. The experimental results were explained with the spin Hamiltonian [11, 12]

$$\mathcal{H}_S = \mu_B(g_{x'}S_{x'}B_{x'} + g_{y'}S_{y'}B_{y'} + g_{z'}S_{z'}B_{z'}) + DS_{z'}^2 + E(S_{x'}^2 - S_{y'}^2) + \tfrac{1}{6}a(S_x^4 + S_y^4 + S_z^4) \qquad (1)$$

with $S = 2$, where D, E and a are the zero-field splitting parameters with their usual meaning, x', y', z' correspond to the orthorhombic axes $[\bar{1}10]$, [001], [110] respectively and x, y, z are the fourfold cubic axes.

As the electronic Zeeman term is of a comparable order of magnitude to the fine structure contributions, exact diagonalization of the Hamiltonian is necessary. The eigenstates of the spin operator $S_{z'}$ are denoted by $|2, m_S\rangle$. In equation (1) and in zero field, the fine structure D-term dominates; it splits the fivefold spin degeneracy into a singlet ($|2, 0\rangle$) and two doublets $\{(|2, +1\rangle, |2, -1\rangle\}$ and $\{|2, +2\rangle, |2, -2\rangle)\}$ at energies D and $4D$ respectively relative to the singlet. From the temperature dependence of the relative intensities of the experimental lines, it was found that D is negative, and thus the $\{|2, +2\rangle, |2, -2\rangle\}$ doublet is lowest in energy. The EPR lines observed were assigned to transitions between the states associated with the upper doublet and with the lower doublet. In general, lines corresponding to the lower doublet were narrower than those associated with the upper doublet. The $|2, 0\rangle \leftrightarrow |2, +1\rangle$ transition was also observed in some orientations at 37 GHz [10].

The superhyperfine (shf) interaction of the 3d electrons of Cr^{2+} with the fluoride nuclei could not be resolved from the CW-EPR spectra. Only a shf structure corresponding to a dominant interaction with four nearest fluoride nuclei could be observed for transitions within the lower doublet and in some high symmetry orientations in the upper doublet as well.

In order to gain an insight into the neighbourhood of the central ion, pulsed EPR experiments were performed on chromium-doped SrF_2 and CaF_2 samples. Electron spin echoes were only detected for Cr^{2+} centres in SrF_2 [11]. In addition, electron spin echo envelope modulation (ESEEM) results allowed more information to be obtained about the superhyperfine interaction in this lattice. A model was proposed for Cr^{2+} in SrF_2 in which the four fluoride ions in the (110) plane relax inwards to touch the chromium ion and the remaining four fluoride ions relax outwards into the next Sr^{2+} ion cage. The hyperfine interaction with the Cr^{2+} nucleus was not resolved. This was because the only isotope with a non-zero nuclear spin ($^{53}Cr^{2+}$, $I = 3/2$) has a low natural abundance (9.5%) and its weak additional hyperfine lines overlap with the shf lines corresponding to the dominant $I = 0$ chromium isotope.

3. A Jahn–Teller theoretical model

A Cr^{2+} ion ($3d^4$) enters a fluorite-type lattice by substituting for the divalent cation at the centre of a halide cube at an eightfold co-ordinated site with cubic symmetry. The cubic crystalline

field splits the ^{5}D free ion term into an orbital doublet ^5E_g and a triplet $^5T_{2g}$, with the latter being the ground state.

The Hamiltonian describing Cr^{2+} impurities in these halides can be written in a general way as

$$\mathcal{H} = \mathcal{H}_{int} + \mathcal{H}_{lat} + \mathcal{H}_{ion} \tag{2}$$

where $\mathcal{H}_{int}$ represents the interaction between Cr^{2+} and the lattice vibrations, $\mathcal{H}_{lat}$ the kinetic and elastic energies for the harmonic lattice and $\mathcal{H}_{ion}$ includes interactions such as spin–orbit coupling and Zeeman terms.

Assuming that Cr^{2+} ions in these lattices are JT systems with strong coupling, the dominant terms in equation (2) will correspond to $\mathcal{H}_{int} + \mathcal{H}_{lat}$. If we take into account the symmetry of the surroundings and the orthorhombic features of the EPR spectra, the JT effect for this ion has to be of $T_{2g} \otimes (e_g + t_{2g})$ type. This problem has been solved in the literature using different approaches. Following the unitary transformation method of Bates *et al* [15] and including quadratic coupling to the lattice, six orthorhombic wells can be obtained as the lowest energy solutions. The six wells are degenerate in energy and correspond to the six possible $\langle 110 \rangle$ distortion directions. Tunnelling between the wells occurs and the ground state corresponds to a $^5T_{2g}$ vibronic triplet and the inversion level to a $^5T_{1g}$ state at a relative energy δ [16]. In the situation of strong coupling but provided δ is large enough, the effect of the interactions included in $\mathcal{H}_{ion}$ can be treated as perturbations on the ground vibronic state. Using the isomorphism between the $^5T_{2g}$ ground state and $l = 1$ states and including the perturbations up to second order, we obtain the effective Hamiltonian [17]

$$\begin{aligned}\mathcal{H}^{(2)}_{eff} = {} & 2\mu_B \boldsymbol{B}\cdot\boldsymbol{S} + \gamma K_1 \boldsymbol{l}\cdot(\lambda\boldsymbol{S} + \mu_B\boldsymbol{B}) + \lambda^2\gamma^2(\tfrac{2}{3}K_2 E(l)E(S) \\ & -\tfrac{1}{2}K_3 \boldsymbol{l}\cdot\boldsymbol{S} + \tfrac{2}{3}K_4 T(l)T(S)) + \lambda\mu_B\gamma^2[\tfrac{2}{3}K_5 l(l+1)(\boldsymbol{B}\cdot\boldsymbol{S}) \\ & +\tfrac{4}{3}K_6 E(l)E(SB) + \tfrac{4}{3}K_7 T(l)T(SB)]\end{aligned} \tag{3}$$

with $\lambda = 57\ \mathrm{cm}^{-1}$ and the isomorphic constant $\gamma = -1$ for the $D(T_2)$ orbital state. The orbital and spin operators are given by the expressions

$$\begin{aligned} E(l)E(S) &= E^l_\theta E^S_\theta + E^l_\varepsilon E^S_\varepsilon & E(l)E(SB) &= E^l_\theta E^{SB}_\theta + E^l_\varepsilon E^{SB}_\varepsilon \\ T(l)T(S) &= T^l_{xy}T^S_{xy} + T^l_{yz}T^S_{yz} + T^l_{zx}T^S_{zx} & T(l)T(SB) &= T^l_x T^{SB}_x + T^l_y T^{SB}_y + T^l_z T^{SB}_z \end{aligned} \tag{4}$$

with

$$E^l_\theta = \frac{1}{2}[3l_z^2 - l(l+1)] \qquad E^l_\varepsilon = \frac{\sqrt{3}}{4}[l_+^2 + l_-^2] \qquad T^l_{yz} = \frac{\sqrt{3}}{2}[l_y l_z + l_z l_y] \qquad \text{etc.} \tag{5}$$

The remaining operators are obtained with l replaced by S and/or B. The coefficient $K_1 \equiv K^{(1)}_{T_1}$ is the first-order reduction factor for orbital operators of T_1 symmetry and the coefficients $K_2 \equiv K_6 \equiv K^{(2)}_E$, $K_3 \equiv K^{(2)}_{T_1}$, $K_4 \equiv K_7 \equiv K^{(2)}_{T_2}$ and $K_5 \equiv K^{(2)}_{A_1}$ are the second-order reduction factors for orbital operators of E, T_1, T_2 and A_1 symmetries respectively. The first-order [18] and second-order [19] vibronic reduction factors have been calculated previously for the strongly coupled orthorhombic $T_{2g} \otimes (e_g + t_{2g})$ JT system.

The effective Hamiltonian in equation (3) was obtained assuming all the excited states were at a sufficiently high energy above the $^5T_{2g}$ state for their effect on the ground state to be ignored. When this interaction cannot be neglected, the total effective Hamiltonian describing the Jahn–Teller system should be obtained by adding to equation (3) the contribution of the other Cr^{2+} states coupled to $^5T_{2g}$ via spin–orbit coupling. This does not add any new terms of different symmetries, but modifies the meaning of the coefficients K_i ($i = 1$ to 7) so that they no longer correspond exclusively to first- and second-order reduction factors. They now include some contributions due to the excited states, so should be regarded as free parameters.

Further contributions to the effective Hamiltonian arise if the basic orbital states are replaced by molecular orbital states. (See, for example, the work of Viccaro *et al* [20] and Zhou and Li [21] related to the GaAs:Cr^{2+} system.) These authors discuss contributions to the spin Hamiltonian parameters and the energies of the system and thus inevitably to the parameters appearing in the effective Hamiltonian given in (3). However, we must point out that we do not agree with the basic assumption made in [20] and [21] that the JT effect is static for GaAs:Cr^{2+}. Nevertheless, a molecular orbital approach combined with the dynamic JT theory presented here earlier should result in an improved model for this system. Unfortunately, as in the case of coupling to the excited states describing above, such a contribution cannot be isolated from the other contributions and again it is merely absorbed into the general expression.

The effective Hamiltonian in equation (3) describes an isolated centre with cubic symmetry when placed in an ideal crystal. However, we are dealing with real crystals in which the ions in the lattice are subjected to internal strains of different magnitude. The effect of strains in strongly coupled orbital triplet JT systems has been previously analysed [22]. On taking into account the orthorhombic symmetry of the Cr^{2+} in these halides, it is reasonable to assume that the system couples more strongly to orthorhombic strains than to strains of other symmetries. When these orthorhombic strains are included in the study, the energy of one orthorhombic well can be lowered by more than that of any other well [22] and the system will show a static orthorhombic distortion. There will be a distribution of sites subject to different strain magnitudes, and so the experimental EPR spectrum will consist of the resonances from ions in all these different strained sites. In principle, the magnetic field values for the EPR resonances would be expected to depend on the strain and so the EPR lines would broaden beyond recognition. However, it is possible for the levels between which a transition occurs to be parallel over a large range of strains in an energy–field plot. Thus, resonances from sites subject to a large range of different strains superimpose. This effect, known as strain stabilization, can explain the experimental observation of narrow and intense peaks.

The Hamiltonian describing the effect of a [110] strain over the vibronic ground state $^5T_{2g}$ can be expressed as [23]

$$\mathcal{H}_{strain} = V(E_\theta \sin\alpha + T_{xy}\cos\alpha) \tag{6}$$

where V represents the effective magnitude of the strain. The parameter α depends on the system considered and determines the direction in the five-dimensional nuclear coordinate space in which the D_{2h} orthorhombic distortion occurs. Appropriate combinations of the orbital operators E_θ, E_ε, T_{xy}, T_{yz} and T_{zx} in equation (6) enable the Hamiltonian for the remaining five orthorhombic directions to be obtained. The Hamiltonian that describes the JT strain-stabilized systems is

$$\mathcal{H} = \mathcal{H}^{(2)}_{eff} + \mathcal{H}_{strain}. \tag{7}$$

The parameters that appear in equation (7) cannot be obtained in a very reliable way from the calculations because many contributions from excited states and from molecular rather than ionic orbitals are present as discussed above. Therefore, values for the parameters will be obtained by fitting the experimental EPR results to the theoretical data calculated using the Hamiltonian $\mathcal{H}$.

4. Results

We first summarize the experimental results obtained previously. Figures 1 and 2 give the isofrequency curves† in the $(\bar{1}10)$ plane showing experimental magnetic field values for the

† The isofrequency curves give the angular dependence of the EPR peaks at a fixed frequency.

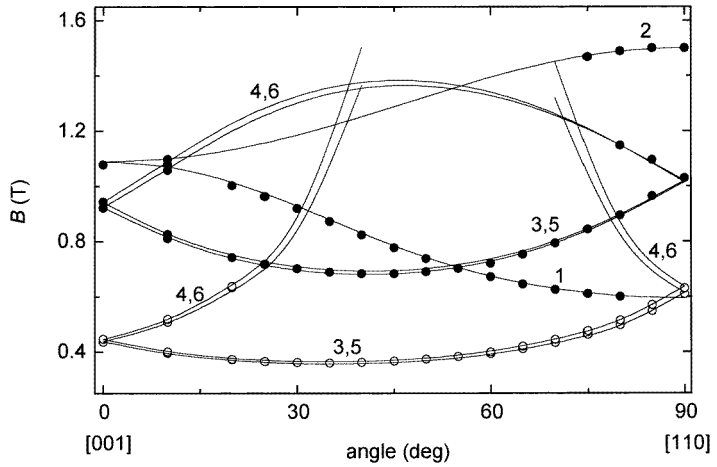

Figure 1. The angular dependence of the EPR line positions of CaF_2:Cr^{2+} for $\boldsymbol{B}$ in the $(\bar{1}10)$ plane measured at a frequency of 34 GHz and a temperature of 10 K. The circles correspond to the experimental points and the solid lines to the theoretical positions calculated using the effective Hamiltonian in equation (7) and parameter values given in equations (8) and (9). The numbers on the curves denote the symmetries of the orthorhombic sites as follows: (1): [110], (2): $[1\bar{1}0]$, (3): [011], (4): $[01\bar{1}]$, (5): [101] and (6): $[\bar{1}01]$.

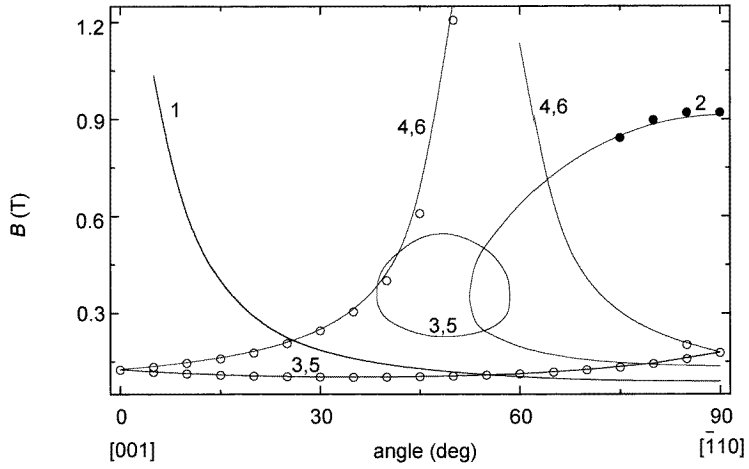

Figure 2. As figure 1 for CaF_2:Cr^{2+} but at a frequency of 9.78 GHz.

EPR resonances measured on CaF_2:Cr crystals at microwave frequencies of 34 GHz and 9.78 GHz respectively. The lines have been labelled with a number 1–6 indicating the direction of the stabilizing strain as defined in the caption of figure 1. Figure 3 gives similar results for SrF_2:Cr crystals at a frequency of 9.78 GHz, whilst figures 4 and 5 give results obtained for SrF_2:Cr crystals in the (111) plane at frequencies of 9.78 GHz and 34 GHz respectively. All experiments were carried out at a temperature of 10 K. In all cases, the solid circles are the experimental points assigned to the resonances within the upper doublet and open circles to those within the lower doublet. (The classification of the resonances to the upper/lower doublet was achieved by additional independent temperature-dependent measurements and by

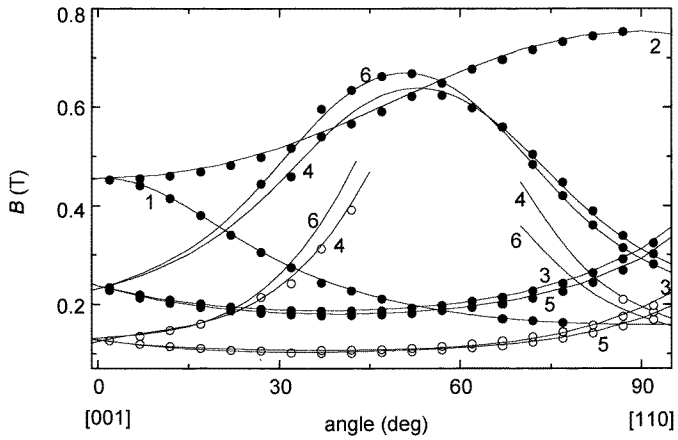

Figure 3. As figure 1 but for SrF_2:Cr^{2+} for $\boldsymbol{B}$ in the $(\bar{1}10)$ plane measured at 9.78 GHz and at 10 K. The circles show the experimental points and the solid lines indicate the corresponding theoretical positions calculated using the effective Hamiltonian given in equation (7) and the parameter values given in equations (9) and (10).

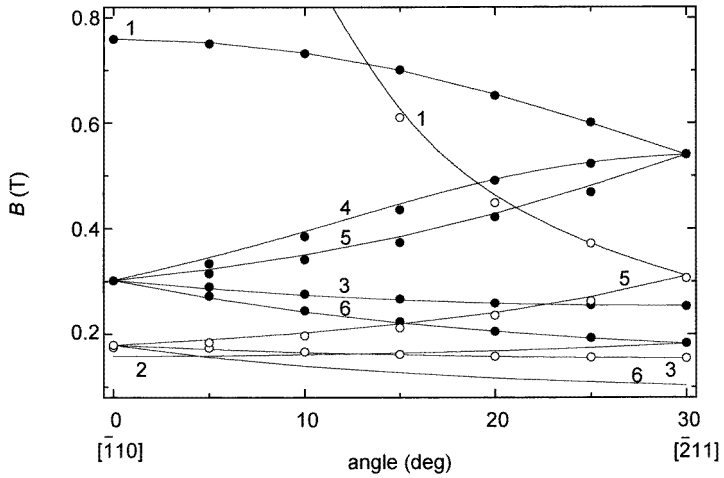

Figure 4. As figure 3 for SrF_2:Cr^{2+} in the (111) plane measured at 9.78 GHz and 10 K.

noting the relative sizes of the resonant fields). Several resonances can be observed in each orientation. They are associated with Cr^{2+} centres stabilized by different orthorhombic strains.

The parameters appearing in the effective Hamiltonian in equation (7) which give the best fit to the data shown in figures 1 and 2 for the CaF_2 system are:

$$\begin{aligned} &K_2 = (8.19 \pm 0.06) \times 10^{-4}\ (\mathrm{cm}^{-1})^{-1} && K_4 = (8.90 \pm 0.06) \times 10^{-4}\ (\mathrm{cm}^{-1})^{-1} \\ &K_5 = -(3.7 \pm 1.2) \times 10^{-4}\ (\mathrm{cm}^{-1})^{-1} && K_6 = (4.7 \pm 4.5) \times 10^{-4}\ (\mathrm{cm}^{-1})^{-1} \\ &K_7 = (2.3 \pm 1.2) \times 10^{-4}\ (\mathrm{cm}^{-1})^{-1} && \alpha = -0.52 \pm 0.07 \text{ for } V \geqslant 85\ \mathrm{cm}^{-1}. \end{aligned} \tag{8}$$

The parameters K_1 and K_3 could not be determined independently, but were found to satisfy the relation

$$K_1 + \frac{\lambda}{2} K_3 = (4.7 \pm 0.3) \times 10^{-2}. \tag{9}$$

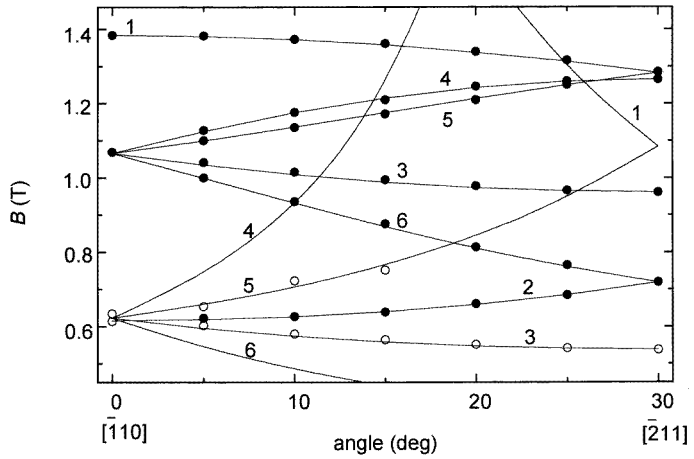

Figure 5. As figure 3 for SrF_2:Cr^{2+} in the (111) plane measured at 34 GHz and 10 K.

Figures 1 and 2 also show the theoretical isofrequency curves computed from these parameter values. However, prior to the running of the actual fitting programmes, it was noticed that the expected coincidence of the isofrequency curves from the $\{3, 5\}$ and $\{4, 6\}$ pairs of sites was broken in some orientations due to a small misalignment. Consequently, the theoretical curves shown in figure 1 were obtained after taking into account a misalignment in the [110] direction corresponding to errors of $\Delta\theta \approx 0.7^\circ$ and $\Delta\varphi \approx 1^\circ$ where θ and φ are the polar and azimuthal angles respectively which should take the values $\theta = 90^\circ$ and $\varphi = 45^\circ$ for the [110] direction.

An equivalent fitting procedure was then followed for the orthorhombic Cr^{2+} centres in SrF_2. In the (111) plane, the six possible orthorhombic distortions can be observed for most of the orientations, as shown in figure 4 and 5 (appropriately labelled). The best set of parameters to describe simultaneously the data at frequencies of 9.78 GHz (figure 4) and 34 GHz (figure 5) is:

$$\begin{aligned} &K_2 = (8.32 \pm 0.07) \times 10^{-4}\ (\mathrm{cm}^{-1})^{-1} && K_4 = (8.64 \pm 0.08) \times 10^{-4}\ (\mathrm{cm}^{-1})^{-1} \\ &K_5 = -(3.2 \pm 0.8) \times 10^{-4}\ (\mathrm{cm}^{-1})^{-1} && K_6 = (2.9 \pm 1.1) \times 10^{-4}\ (\mathrm{cm}^{-1})^{-1} \\ &K_7 = (2.7 \pm 0.7) \times 10^{-4}\ (\mathrm{cm}^{-1})^{-1} && \alpha = -0.49 \pm 0.03 \text{ for } V \geqslant 300\ \mathrm{cm}^{-1}. \end{aligned} \tag{10}$$

Once more, the parameters K_1 and K_3 satisfy equation (9) within the uncertainties quoted. These parameter values gave the theoretical isofrequency curves in the $(\bar{1}10)$ plane drawn in figure 3. As in the case of Cr^{2+} in CaF_2, a misalignment was observed in this plane that corresponded to an angle variation of $\Delta\theta \approx 0.85^\circ$ and $\Delta\varphi \approx 3^\circ$ with respect to the [110] direction. The agreement between the experimental data and the magnetic field values obtained from the exact diagonalization of the Hamiltonian in equation (7) and the set of parameters in equation (10) is excellent.

Although the model given above appears to fit the observed data well, it will only be applicable if it results in strain-stabilized transitions in order to explain the narrow resonances observed. We therefore plot the energy of the vibronic $^5T_{2g}$ ground state as a function of the strain energy V obtained from an act diagonalization of the Hamiltonian in equation (7) and the parameter set obtained above for CaF_2:Cr^{2+} in equation (8) for the special case of zero field. This is presented in figure 6; the transformation properties of the levels are given for zero strain that correspond to O_h symmetry. The levels in finite strain are all singlets, because of

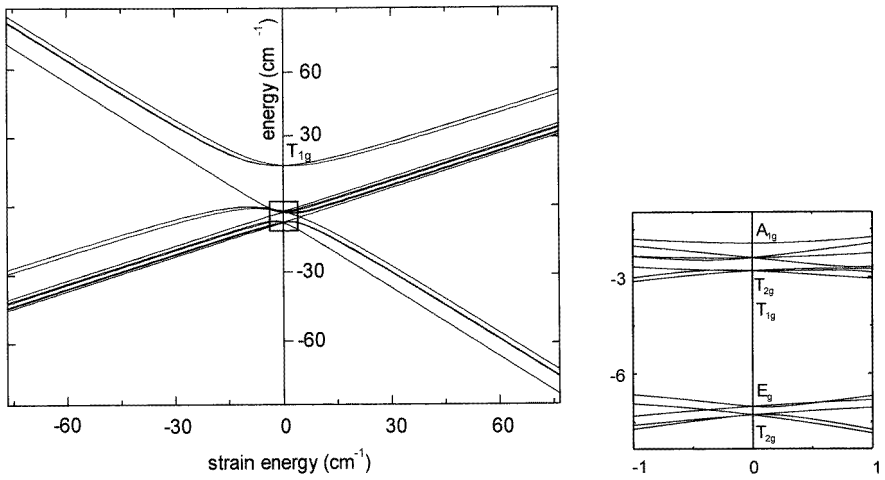

Figure 6. Energy level diagram for a $^5T_{2g}$ vibronic ground state in zero magnetic field as a function of strain obtained using the effective Hamiltonian in equation (7) and the parameter values given in equations (8) and (9). The labelling of the levels denotes the transformation properties under the D_{2h} group.

the reduction in symmetry, although some of the singlets are accidentally degenerate. If V is taken large enough, it can be see that the energy levels remain parallel for a large range of strain magnitudes. Moreover, positive strains isolate a lower set of five states consisting of one singlet and two nearly degenerate doublets. For $V > 300$ cm^{-1} the lowest state is nearly a doublet and the following two states are at an energy of about $3|D|$ higher (with $|D| \sim 2.8$ cm^{-1})) and separated by 0.36 cm^{-1}. The upper state is a singlet having an energy of about $4|D|$ above the lower doublet. The orbital contribution to these states corresponds approximately to a $(|1, +1_l\rangle - \mathrm{i}|1, -1_l\rangle)$ state where $|1, m_l\rangle$ are the eigenstates of the orbital operator l_z with $l = 1$. As expected, this state corresponds to the orbital state $|x + y\rangle$ for an orthorhombic distortion along the [110] direction. The electronic spin state is a linear combination of $|2, m_s\rangle$ spin states where $|2, m_s\rangle$ are the eigenstates of the spin operator $S_{z'}$. The lowest doublet is built from the $|2, \pm 2\rangle$ spin states, the upper doublet from a linear combination of $|2, \pm 1\rangle$ spin states and the singlet corresponds to the $|2, 0\rangle$ spin state. Assuming that the orthorhombic strain stabilizes the five lowest states, the picture obtained from the effective Hamiltonian given in equation (7) is very similar to the scheme obtained using the static spin Hamiltonian of equation (1).

5. Discussion and conclusions

We have proposed an effective Hamiltonian to describe Cr^{2+} centres in both SrF_2 and CaF_2. Values for the parameters appearing in this effective Hamiltonian have been determined that give a good fit to the experimental data. This in turn justifies the neglect of admixtures of the tunnelling level into the ground state via the perturbations of spin–orbit coupling and strain as δ is large. We can observe a similarity between the parameter sets in equations (8) and (10) that fit the EPR spectra for Cr^{2+} in two different alkaline earth halides. The parameters for the terms describing the effect of the spin–orbit coupling could be determined quite accurately. However, the theoretical magnetic fields for the EPR resonances were more insensitive to the values of the parameters appearing in the Zeeman terms and so they have a greater uncertainty.

More detailed calculations show that the resonances assigned to the ground state doublet are strain stabilized for lower magnitudes of the strain ($V \sim 65$ cm^{-1}) than those within the upper doublet ($V \sim 85$ cm^{-1} in CaF_2, $V \sim 300$ cm^{-1} in SrF_2). This suggests that more strained sites contribute to the spectra from the lower doublet compared with the upper doublet. Taking into account this result, some previous analyses should be revisited. Oliete *et al* [11, 12] determined the magnitude of the parameter a appearing in equation (1) from the ratio of the intensities of transitions in the two doublets. As the value of $|a|$ is increased, the calculated intensity of the transition within the lower doublet increases. However, if more Cr^{2+} centres contribute to the lower doublet spectra, the intensity will also increase. The value obtained above for $|a|$ will represent therefore an upper bound only. Therefore, the determination of parameters involving the experimental intensities of the EPR lines in these kind of strain-stabilized systems should be performed with great care.

The theoretical magnetic field values for the EPR resonances were obtained from the exact diagonalization of the Hamiltonian in equation (7). The fitting to the experimental results was attempted taking as $\mathcal{H}^{(2)}_{eff}$ the Hamiltonian in equation (3). In both lattices, it is necessary to treat the coefficients of the terms in the effective Hamiltonian as free parameters, rather than restricting them to specific first- and second-order reduction factors. In addition, the signs of most of the parameters that fitted the EPR spectra were positive. Hallam *et al* [19] derived expressions for the second-order vibronic reduction factors for the strongly coupled $T_{2g} \otimes (e_g + t_{2g})$ Jahn–Teller system, and found that the signs of $K^{(2)}_E$, $K^{(2)}_{T_1}$, $K^{(2)}_{T_2}$ and $K^{(2)}_{A_1}$ were all negative. Both of these facts lead to the conclusion that the coupling of the ground state to the excited state in these systems and molecular orbital-type contributions should not be totally neglected. Due to the absence of optical data in these fluorides, it is difficult to carry out a more complete analysis to determine the main states that contribute to the Hamiltonian and the sizes of their contributions. This is not the first time that it has been necessary to include the coupling to the excited states in order to explain the features observed experimentally in JT centres. Previously, Parker *et al* [23] described a model for the orthorhombic Cr^{3+} centres in GaAs in which the closeness of the first excited ^2E state of the ion to the $^4T_1$ ground state caused much admixing.

The effective Hamiltonian derived from the theoretical Jahn–Teller model for Cr^{2+} in CaF_2 and SrF_2 succeeds in describing these orthorhombic systems better than the spin Hamiltonian used by Oliete and co-workers [11, 12]. The intense EPR resonances come from ions in orthorhombically strain-stabilized sites which generate the static features of the spectra. An EPR strain-stabilized spectrum has been identified previously for other Cr^{2+} JT systems namely for GaAs:Cr^{2+} [7] and InP:Cr^{2+} [24]. However, in these systems, the ion occupies a site of tetragonal symmetry. To our knowledge, the crystals studied here are the first to show a divalent chromium ion in an orthorhombically distorted site.

Acknowledgments

One of us (PBO) thanks the European Community for a Training and Mobility Research Marie Curie grant. We also thank Dr Y-M Liu for many helpful discussions.

References

[1] Baranowski J M 1986 *Deep Centers in Semiconductors* ed S T Pantelides (New York: Gordon and Breach) p 691
[2] Krebs J J and Stauss G H 1977 *Phys. Rev.* B **16** 971
[3] Stauss G H, Krebbs J J and Henry R L 1977 *Phys. Rev.* B **16** 974

[4] Vallin J T and Watkins G D 1974 *Phys. Rev.* B **9** 2051
[5] Dziesiaty J, Peka P, Lehr M U, Klimakow A, Müller S and Schulz H-J 1997 *Z. Phys. Chem.* **201** 63
[6] Krebs J J and Stauss G H 1979 *Phys. Rev.* B **20** 795
[7] Abhvani A S, Austen S P, Bates C A, Parker L W and Pooler D R 1982 *J. Phys. C: Solid State Phys.* **15** 2217
[8] Ulrici W 1977 *Phys. Status Solidi* b **84** K155
[9] Oliete P B, Orera V M and Alonso P J 1996 *J. Phys.: Condens. Matter* **8** 6797
[10] Zaripov M M, Tarasov V F, Ulanov V A, Shajkurov G S and Popov M L 1995 *Sov. Phys.–Solid State* **38** 249
[11] Oliete P B, Orera V M and Alonso P J 1996 *Phys. Rev.* B **54** 12 099
[12] Oliete P B, Orera V M and Alonso P J 1995 *Phys. Rev.* B **53** 3047
[13] Zaripov M M, Ulanov V A, Shakurov G S and Tarasov V F 1996 *Symp. on Electrons and Vibrations in Solids and Finite Systems (Berlin, 1996)*
[14] Oliete P B, Orera V M and Aonso P J 1998 *Appl. Magn. Reson.* **15** 155
[15] Bates C A, Dunn J L and Sigmund E 1987 *J. Phys.: Solid State Phys.* **20** 1965
[16] Dunn J L and Bates C A 1989 *J. Phys.: Condens. Matter* **1** 375
[17] Liu Y M 1995 *Thesis* University of Nottingham, Department of Physics
[18] Dunn J L and Bates C A 1989 *J. Phys.: Condens. Matter* **1** 2617
[19] Hallam L D, Dunn J L and Bates C A 1992 *J. Phys.: Condens. Matter* **4** 6797
[20] Viccaro M H de A, Sundaram S and Sharma R R 1982 *Phys. Rev.* B **25** 7731
[21] Zhou Y-Y and Li F-Z 1995 *Phys. Rev.* B **51** 14 176
[22] Dunn J L and Bates C A 1988 *J. Phys.: Solid State Phys.* **21** 2495
[23] Parker L W, Bates C A, Dunn J L, Vasson A and Vasson A-M 1990 *J. Phys.: Condens. Matter* **2** 2841
[24] Handley J, Bates C A, Vasson A, Vasson A-M, Ferdjani K and Tebbal N 1990 *Semicond. Sci. Technol.* **5** 710